Two-Terminal Numerical Algorithm for Single-Phase Arcing Fault Detection and Fault Location Estimation Based on the Spectral Information

Hyun-Houng Kim*, Chan-Joo Lee, Jong-Bae Park*, Joong-Rin Shin† and Sang-Yun Jeong***

Abstract – This paper presents a new numerical algorithm for the fault location estimation and arcing fault detection when a single-phase arcing ground fault occurs on a transmission line. The proposed algorithm derived in the spectrum domain is based on the synchronized voltage and current samples measured from the PMUs (Phasor Measurement Units) installed at both ends of the transmission lines. In this paper, the algorithm uses DFT (Discrete Fourier Transform) for estimation. The algorithm uses a short data window for real-time transmission line protection. Also, from the calculated arc voltage amplitude, a decision can be made whether the fault is permanent or transient. The proposed algorithm is tested through computer simulation to show its effectiveness.

Keywords: Fault location, Numerical algorithms, Protection, Spectrum-domain, With/without shunt capacitance

1. Introduction

In the competitive electricity market, a rapid fault restoration on a transmission line is faced with the quality of a utility's power service. From the viewpoints of economics and power system quality, the importance of fault detection and location of transmission lines is increased. The fast and accurate determination of fault location on electric power transmission lines has been utilized as an aid in fault analysis and power restoration. At the same time, the fault determination adversely impacts service reliability, operation costs, and the quality of power delivery. Therefore, to aid the rapid and efficient service restoration, an accurate fault location estimation and fault discrimination technique are needed.

To improve the computation of fault location, many authors have suggested utilizing the information from both line ends. M. Kezunovc et al. proposed a fault location algorithm based on synchronized sampling technique [1]. The authors adopted a time domain model of a transmission line as a basis for the algorithm development. The accuracy of the proposed algorithm is well within 1% error, however, the data must be acquired at a sufficiently high sampling rate to provide adequate approximation of the derivatives, which depend heavily on the selection of the line model and system itself. A.A. Girgis et al. proposed another fault location algorithm based upon two-end data [2]. While the authors considered the synchronization errors in sampling the voltage and current waveforms at different line terminals, the line models employed are lump-types, which cannot really reflect the effect of inter-phase coupling phenomenon. D. Novosel et al. proposed the two-terminal fault location estimation approaches based on unsynchronized data [3]. In this paper the authors utilized the lump-model to represent the short line and made compensation for long lines. The described schemes suit only off-line post fault analysis. Recently, advanced technology progress such as GPS (Global Positioning System) has helped us to provide more accurate computations. Many studies for a fault location/detection technique using the GPS have been carried out [4-6].

In this paper, a new two-terminal algorithm for fault location estimation and arcing detection is derived in the spectrum domain. The proposed algorithms are based on the only use of voltage and current samples that are synchronously taken from assumed PMUs installed at both ends of a transmission line. Also, the arc voltage wave shape is modeled numerically on the basis of a great number of arc voltage records. From the calculated arc voltage amplitude it can make a decision as to whether the fault is permanent or transient.

2. Fault algorithm in spectrum domain

In this paper, a new two-terminal numerical algorithm for fault location estimation and fault recognition is

† Corresponding Author: Dept. of Electrical Engineering, Konkuk University, Korea. (jrshin@konkuk.ac.kr)
* Dept. of Electrical Engineering, Konkuk University, Korea
** K-Power Co. Ltd., Korea
Received 13 June, 2008 ; Accepted 2 October, 2008

derived in spectrum domain. Based on the length of the transmission line, two types of algorithms are developed as follows:

- Short line algorithm without shunt capacitance
- Long line algorithm with shunt capacitance

The developed algorithms are based on the synchronized phasors obtained by assumed PMUs installed at both terminals of the transmission lines.

2.1 Short line application

The short line algorithm is suitable for transmission lines that are less than 80 ㎞. To derive the short line algorithm, it assumes that an a-phase arcing ground fault occurs on the transmission lines at ℓ away from the sending end as shown in Fig. 1. Due to the short transmission line, the shunt capacitance and conductance of the transmission line will be neglected. In Fig. 1, all variables have radian frequency ($h\omega$) and all line parameters are calculated in terms of $h\omega$. The fault point is denoted by F at a distance, ℓ, from the sending end, (S). Here, index h denotes the order of harmonic, D is line length, and subscripts S and R correspond to the sending- and receiving end of the line, respectively. Shunt capacitance will be neglected for the initial discussion.

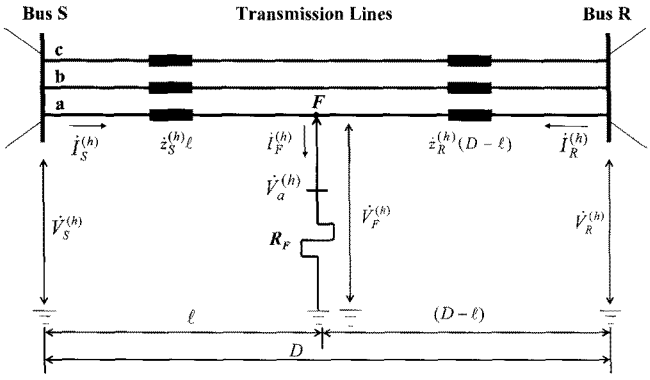

Fig. 1. Three phase transmission line with phase-a to ground fault.

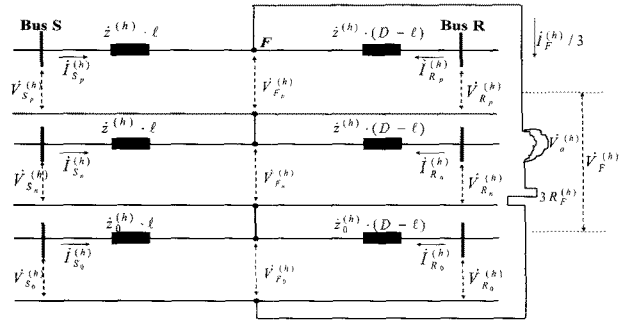

Fig. 2. Equivalent sequence network connection of faulted line

The three phase circuit from Fig. 1 can be presented by the three single-phase equivalent sequence circuits of the faulted lines as shown in Fig. 2. The three single-phase equivalent circuits are positive (p), negative (n), and zero (0) sequence circuits, respectively.

For the equivalent sequence network depicted in Fig. 2, the following equations can be obtained:

$$\begin{aligned}\dot{V}_{S_p}^{(h)} &= \dot{z}^{(h)}\ell\dot{I}_{S_p}^{(h)} + \dot{V}_{F_p}^{(h)},\\ \dot{V}_{S_n}^{(h)} &= \dot{z}^{(h)}\ell\dot{I}_{S_n}^{(h)} + \dot{V}_{F_n}^{(h)},\\ \dot{V}_{S_0}^{(h)} &= \dot{z}_0^{(h)}\ell\dot{I}_{S_0}^{(h)} + \dot{V}_{F_0}^{(h)}\end{aligned} \tag{1}$$

$$\begin{aligned}\dot{V}_{R_p}^{(h)} &= \dot{z}^{(h)}(D-\ell)\dot{I}_{R_p}^{(h)} + \dot{V}_{F_p}^{(h)},\\ \dot{V}_{R_n}^{(h)} &= \dot{z}^{(h)}(D-\ell)\dot{I}_{R_n}^{(h)} + \dot{V}_{F_n}^{(h)},\\ \dot{V}_{R_0}^{(h)} &= \dot{z}_0^{(h)}(D-\ell)\dot{I}_{R_0}^{(h)} + \dot{V}_{F_0}^{(h)}\end{aligned} \tag{2}$$

where,

$\dot{V}_{S_{p,n,0}}^{(h)}, \dot{V}_{R_{p,n,0}}^{(h)}$: positive-, negative-, and zero sequence phase voltage of the h-th harmonic at both ends of the lines,

$\dot{I}_{S_{p,n,0}}^{(h)}, \dot{I}_{R_{p,n,0}}^{(h)}$: positive-, negative-, and zero sequence phase voltage of the h-th harmonic at both ends of the lines,

$\dot{V}_{F_{p,n,0}}^{(h)}$: positive-, negative-, and zero sequence faulted phase voltage of the h-th harmonic at the fault point,

$\dot{z}^{(h)}$: positive- or negative- sequence line impedance for the h-th harmonic,

$\dot{z}_0^{(h)}$: zero sequence line impedance for the h-th harmonic.

By adding the above equations, and using the basic symmetrical component equations, the phase voltage and current of the h-th harmonic can be obtained:

$$\dot{V}_S^{(h)} = \dot{V}_{S_p}^{(h)} + \dot{V}_{S_n}^{(h)} + \dot{V}_{S_0}^{(h)},\quad \dot{I}_S^{(h)} = \dot{I}_{S_p}^{(h)} + \dot{I}_{S_n}^{(h)} + \dot{I}_{S_0}^{(h)} \tag{3}$$

$$\dot{V}_R^{(h)} = \dot{V}_{R_p}^{(h)} + \dot{V}_{R_n}^{(h)} + \dot{V}_{R_0}^{(h)},\quad \dot{I}_R^{(h)} = \dot{I}_{R_p}^{(h)} + \dot{I}_{R_n}^{(h)} + \dot{I}_{R_0}^{(h)} \tag{4}$$

$$\dot{V}_F^{(h)} = \dot{V}_{F_p}^{(h)} + \dot{V}_{F_n}^{(h)} + \dot{V}_{F_0}^{(h)} \tag{5}$$

The phase voltage of the h-th harmonic at the sending- and receiving end is given by:

$$\dot{V}_S^{(h)} = \dot{z}^{(h)}(\dot{I}_S^{(h)} + \dot{k}_z^{(h)}\dot{I}_{S_0}^{(h)})\ell + \dot{V}_F^{(h)} \tag{6}$$

$$\dot{V}_R^{(h)} = \dot{z}^{(h)}(\dot{I}_R^{(h)} + \dot{k}_z^{(h)}\dot{I}_{R_0}^{(h)})(D-\ell) + \dot{V}_F^{(h)} \tag{7}$$

where, $\dot{k}_z^{(h)} = (\dot{z}_0^{(h)} - \dot{z}^{(h)})/\dot{z}^{(h)}$ is the zero sequence compensation factor, which can be calculated in advance.

In this algorithm only fundamental and third harmonic fault model will be used for the algorithm development

because minimal number of harmonics needed for algorithm development is the first and third harmonic.

2.1.1 Fault location calculation

Subtracting (7) from (6), one equation for fundamental harmonic can be obtained:

$$\dot{V}_S^{(1)} - \dot{V}_R^{(1)} = \dot{z}^{(1)}(\dot{I}_S^{(1)} + \dot{k}_z^{(1)}\dot{I}_{S_0}^{(1)})\ell - \dot{z}^{(1)}(\dot{I}_R^{(1)} + \dot{k}_z^{(1)}\dot{I}_{R_0}^{(1)})(D-\ell) \quad (8)$$

The fault distance ℓ from (8) can be calculated as follows:

$$\ell = [\dot{V}_S^{(1)} - \dot{V}_R^{(1)} + \dot{z}^{(1)}(\dot{I}_R^{(1)} + \dot{k}_z^{(1)}\dot{I}_{R_0}^{(1)})D] / \{\dot{z}^{(1)}[\dot{I}_S^{(1)} + \dot{I}_R^{(1)} + \dot{k}_z^{(1)}(\dot{I}_{S_0}^{(1)} + \dot{I}_{R_0}^{(1)})]\} \quad (9)$$

Equation (9) is the explicit fault location expression for the *a*-phase arcing ground fault on transmission line.

2.1.2 Arc voltage amplitude calculation

After calculating the fault distance ℓ from (9), the fault voltage of the third harmonic can be calculated from (5). In [7] the fault resistance R_F can be expressed as follows:

$$R_F = (\dot{V}_F^{(3)} - \dot{k}^{(3)}V_a) / \dot{I}_F^{(3)},\ \dot{k}^{(3)} = \frac{4}{\pi}\frac{1}{3}\angle 3\varphi_1 \quad (10)$$

where, $\dot{k}^{(3)}$ is the coefficient of third harmonic and φ_1 is the phase angle of the fundamental harmonic.

Since the fault resistance is a scalar, equation (10) is expressed as follows:

$$\mathrm{Im}\{R_F\} = \mathrm{Im}\{(\dot{V}_F^{(3)} - \dot{k}^{(3)}V_a) / \dot{I}_F^{(3)}\} = 0 \quad (11)$$

$$\mathrm{Im}\{\dot{V}_F^{(3)} / \dot{I}_F^{(3)}\} - \mathrm{Im}\{\dot{k}^{(3)} / \dot{I}_F^{(3)}\}V_a = 0 \quad (12)$$

The unknown arc voltage amplitude from (12) is calculated as follows.

$$V_a = \mathrm{Im}\{\dot{V}_F^{(3)} / \dot{I}_F^{(3)}\} / \mathrm{Im}\{\dot{k}^{(3)} / \dot{I}_F^{(3)}\} \quad (13)$$

The calculated arc voltage amplitude is used to decide a fault type. A fault is an arcing transient fault if calculated value of arc voltage amplitude is greater than product of arc voltage gradient and the length of the arc path, which is equal or greater than the flashover length of a suspension insulator string. The average arc voltage gradient lies between 12 and 15 V/cm [8].

2.2 Long line application

For lines longer than 250 km, the shunt capacitance of the line, which was previously ignored, has to be accounted for in the line model. If the fault location algorithm does not compensate for shunt capacitance in the long line model, error may be increased to the longer lines on higher voltage levels. In this paper, the distributed line model is used for the development of fault location and discrimination algorithm for long line applications. The line $\prod$ model may be corresponded to the distributed *ABCD* model. The line $\prod$ model is shown in Fig. 3. Here, the unknown ℓ^* is the fault distance away from sending end considering the shunt capacitance and shunt admittance, $\dot{y}^{(h)}$.

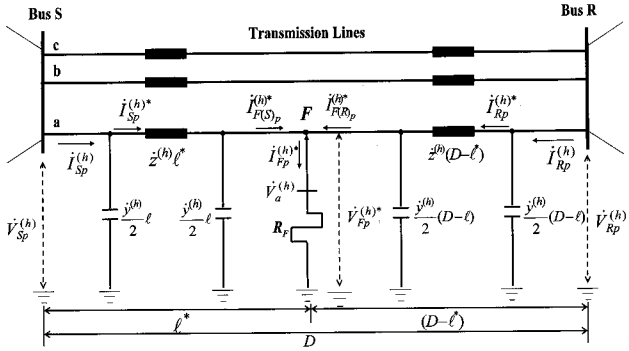

Fig. 3. Schematic diagram line of the faulted system with shunt capacitances.

The fault location algorithm derived without shunt capacitance is approximately expressed as follows:

$$\ell \cong (\dot{V}_{S_p}^{(h)} - \dot{V}_{R_p}^{(h)} + \dot{z}^{(h)}\dot{I}_{R_p}^{(h)}D) / \{\dot{z}^{(h)}(\dot{I}_{S_p}^{(h)} + \dot{I}_{R_p}^{(h)})\} \quad (14)$$

From Fig. 3 the positive sequence phase current of the *h*-th harmonic at both terminals of the lines can be obtained as follows:

$$\dot{I}_{S_p}^{(h)*} = \dot{I}_{S_p}^{(h)} - \dot{V}_{S_p}^{(h)}(\dot{y}^{(h)}/2)\ell \quad (15)$$

$$\dot{I}_{R_p}^{(h)*} = \dot{I}_{R_p}^{(h)} - \dot{V}_{R_p}^{(h)}(\dot{y}^{(h)}/2)(D-\ell) \quad (16)$$

where, $\dot{I}_{S_p}^{(h)*}$ and $\dot{I}_{R_p}^{(h)*}$ are the positive sequence phase current of the *h*-th harmonic in the series impedance at the sending- and receiving ends, respectively.

From KVL the positive sequence phase voltage of the *h*-th harmonic at sending- and receiving ends is given by:

$$\dot{V}_{S_p}^{(h)} = \dot{z}^{(h)}\dot{I}_{S_p}^{(h)*}\ell^* + \dot{V}_{F_p}^{(h)*} \quad (17)$$

$$\dot{V}_{R_p}^{(h)} = \dot{z}^{(h)}\dot{I}_{R_p}^{(h)*}(D-\ell^*) + \dot{V}_{F_p}^{(h)*} \quad (18)$$

The positive sequence faulted phase voltage and current of the *h*-th harmonic are given by:

$$\dot{V}_{F_p}^{(h)} = \dot{V}_{S_p}^{(h)} - \dot{I}_{S_p}^{(h)*}\dot{z}^{(h)}\ell^* \quad (19)$$

$$\dot{I}_{F_p}^{(h)*} = \dot{I}_{F(S)_p}^{(h)*} + \dot{I}_{F(R)_p}^{(h)*} = \dot{I}_{S_p}^{(h)*} + \dot{I}_{R_p}^{(h)*} - \dot{V}_{F_p}^{(h)*}(\dot{y}^{(h)}/2)\ell \quad (20)$$

where, $\dot{I}_{F(S)_p}^{(h)*}$ and $\dot{I}_{F(R)_p}^{(h)*}$ are the positive sequence faulted phase current at sending- and receiving ends of the lines, respectively.

From the equivalent sequence network, the following equations can be obtained:

$$\dot{V}_{F_p}^{(h)*} = \dot{V}_{S_p}^{(h)} - \dot{z}^{(h)}\ell^*\left[\dot{I}_{S_p}^{(h)} - V_{S_p}^{(h)}(\dot{y}^{(h)}/2)\ell^*\right] \quad (21)$$

$$\dot{V}_{F_n}^{(h)*} = \dot{V}_{S_n}^{(h)} - \dot{z}^{(h)}\ell^*\left[\dot{I}_{S_n}^{(h)} - V_{S_n}^{(h)}(\dot{y}^{(h)}/2)\ell^*\right] \quad (22)$$

$$\dot{V}_{F_0}^{(h)*} = \dot{V}_{S_0}^{(h)} - \dot{z}_0^{(h)}\ell^*\left[\dot{I}_{S_0}^{(h)} - V_{S_0}^{(h)}(\dot{y}^{(h)}/2)\ell^*\right] \quad (23)$$

$$\dot{I}_{F_p}^{(h)*} = \dot{I}_{S_p}^{(h)} + \dot{I}_{R_p}^{(h)} - (\dot{y}^{(h)}/2)\left[(\dot{V}_{S_p}^{(h)} - \dot{V}_{R_p}^{(h)})\ell^* + (\dot{V}_{R_p}^{(h)} + \dot{V}_{F_p}^{(h)})D\right] \quad (24)$$

$$\dot{I}_{F_n}^{(h)*} = \dot{I}_{S_n}^{(h)} + \dot{I}_{R_n}^{(h)} - (\dot{y}^{(h)}/2)\left[(\dot{V}_{S_n}^{(h)} - \dot{V}_{R_n}^{(h)})\ell^* + (\dot{V}_{R_n}^{(h)} + \dot{V}_{F_n}^{(h)})D\right] \quad (25)$$

$$\dot{I}_{F_0}^{(h)*} = \dot{I}_{S_0}^{(h)} + \dot{I}_{R_0}^{(h)} - (\dot{y}_0^{(h)}/2)\left[(\dot{V}_{S_0}^{(h)} - \dot{V}_{R_0}^{(h)})\ell^* + (\dot{V}_{R_0}^{(h)} + \dot{V}_{F_0}^{(h)})D\right] \quad (26)$$

where,

$\dot{V}_{F_{p,n,0}}^{(h)*}$: positive-, negative-, and zero sequence faulted phase voltage of the h-th harmonic,

$\dot{I}_{F_{p,n,0}}^{(h)*}$: positive-, negative-, and zero sequence faulted phase current of the h-th harmonic,

$\dot{y}^{(h)}$: positive- or negative sequence line shunt admittance for the h-th harmonic,

$\dot{y}_0^{(h)}$: the zero sequence line shunt admittance for the h-th harmonic.

By adding the above equations, and using the basic symmetrical component equations, the faulted phase voltage and current of the h-th harmonic can be obtained:

$$\dot{V}_F^{(h)*} = \dot{V}_{F_p}^{(h)*} + \dot{V}_{F_n}^{(h)*} + \dot{V}_{F_0}^{(h)*} \quad (27)$$

$$\dot{I}_F^{(h)*} = \dot{I}_{F_p}^{(h)*} + \dot{I}_{F_n}^{(h)*} + \dot{I}_{F_0}^{(h)*} \quad (28)$$

Using the above equations, the fault location and discrimination algorithm can be derived in long line model.

2.2.1 Fault location calculation

Subtracting (27) from (28), one equation for fundamental harmonic can be obtained:

$$\dot{V}_{S_p}^{(1)} - \dot{V}_{R_p}^{(1)} = \dot{z}^{(1)}\left[\dot{I}_{S_p}^{(1)*}\ell^* - \dot{I}_{R_p}^{(1)*}(D - \ell^*)\right] \quad (29)$$

The fault distance, ℓ^*, from (29) can be calculated as follows:

$$\ell^* = \frac{\dot{V}_{S_p}^{(1)} - \dot{V}_{R_p}^{(1)} + \dot{z}^{(1)}\left[\dot{I}_{R_p}^{(1)} - \dot{V}_{R_p}^{(1)}\frac{\dot{y}}{2}(D-\ell)\right]D}{\dot{z}^{(1)}\left[\dot{I}_{S_p}^{(1)} + \dot{I}_{R_p}^{(1)} + \frac{\dot{y}}{2}(\dot{V}_{R_p}^{(1)} - \dot{V}_{S_p}^{(1)} - \dot{V}_{R_p}^{(1)}D)\ell\right]} \quad (30)$$

Equation (30) is the explicit fault location expression in a long line model for the a-phase arcing ground fault on transmission lines.

2.2.2 Arc voltage amplitude calculation

From Fig. 2 the fault voltage of the third harmonic considering the shunt capacitance of the lines can be redefined by the next relation:

$$\dot{V}_F^{(3)*} = R_F\dot{I}_F^{(3)*} + \dot{V}_a = R_F\dot{I}_F^{(3)*} + k^{(3)*}V_a \quad (31)$$

where, $\dot{k}^{(3)*} = k^{(3)}\angle 3\varphi_1^*$ and $\varphi_1^* = ang\{\dot{I}_{F_p}^{(1)*}\}$

$\dot{k}^{(3)*}$: the coefficient of the third harmonic,

φ_1^* : the phase angle for the fundamental harmonic.

From (31), the fault resistance R_F can be expressed as follows:

$$R_F = (\dot{V}_F^{(3)*} - \dot{k}^{(3)*}V_a)/\dot{I}_F^{(3)*} \quad (32)$$

Since the fault resistance is scalar, equation (32) is expressed as follows:

$$\begin{aligned}&\mathrm{Im}\{R_F\} = \mathrm{Im}\left\{(\dot{V}_F^{(3)*} - \dot{k}^{(3)*}V_a)/\dot{I}_F^{(3)*}\right\} = 0\\ &\rightarrow \mathrm{Im}\left\{\dot{V}_F^{(3)*}/\dot{I}_F^{(3)*}\right\} - \mathrm{Im}\left\{\dot{k}^{(3)*}/\dot{I}_F^{(3)*}\right\}V_a = 0\end{aligned} \quad (33)$$

The unknown parameter arc voltage amplitude from (33) can be calculated as follows:

$$V_a = \mathrm{Im}\left\{\dot{V}_F^{(3)*}/\dot{I}_F^{(3)*}\right\}/\mathrm{Im}\left\{\dot{k}^{(3)*}/\dot{I}_F^{(3)*}\right\} \quad (34)$$

3. Case Studies

To test the validity of the proposed algorithms for the fault location estimation and arcing fault detection, the test was performed as shown in Fig. 4. The data for testing was obtained from simulating the system using the Electromagnetic Transients Program (EMTP) under various fault type and parameter scenarios.

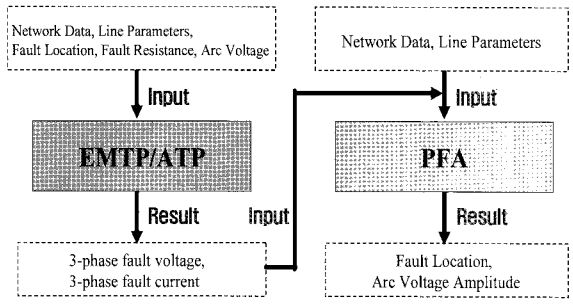

* PFA: The Proposed Fault Algorithm

Fig. 4. Simulation procedure

In this paper, the fault location error to evaluate the algorithm accuracy, in percentage terms, is calculated using the following equation:

$$error[\%] = |(\ell_c - \ell_a)/D| \times 100 \quad (35)$$

where, ℓ_c and ℓ_a represent the calculated fault location and actual location, respectively, and D denotes the whole line length.

3.1 Short line application (without shunt capacitance)

The tests have been done using the Electromagnetic Transient Program (EMTP). The schematic diagram of the 400 [kV] power system on which the tests are based is shown in Fig. 5. Fig. 5 presents the schematic diagram of the synchronized test power system.

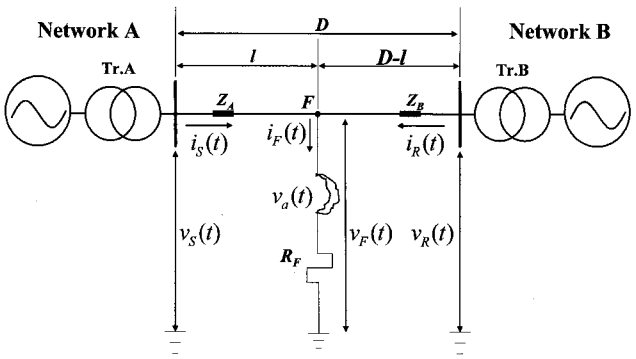

Fig. 5. Schematic of the test power system without shunt capacitance

Here, $v(t)$, $i(t)$, $v_{S,R}(t)$, and $i_{S,R}(t)$ are the digitized voltages and currents, and D is the line length. The line parameters are D =100 [km], r =0.0325 [Ω/km], x=0.36 [Ω/km], r_0 =0.0975 [Ω/km], and x_0 =1.08 [Ω/km]. Data for network A are: R_A =1 [Ω], L_A =0.064[H], R_{A0} =2 [Ω], and L_{A0} =0.128[H]. Data for network B are: R_B =0.5 [Ω], L_B =0.032[H], R_{B0} =1 [Ω], and L_{B0} =0.064[H]. The equivalent electromotive forces of networks A and B are E_A=400[kV] and E_B=395[kV], respectively. Here, network A and B are equivalent power systems connected to sending- and receiving ends of the transmission line, respectively.

Figs. 6, 7, 8, and 9 show the faulted phase voltages and currents at each end of the transmission line, sampled with the sampling frequency f_s =3,840 $Hz(64\ sample/T_0)$ for the single phase to ground fault with arc. The fault is initiated at 10% of the line.

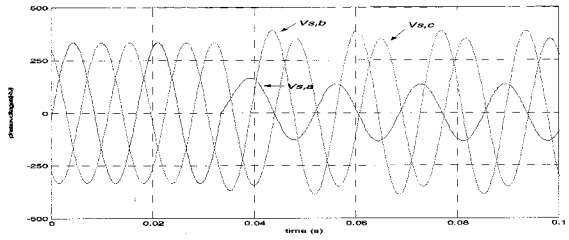

Fig. 6. Faulted phase voltages at the sending end

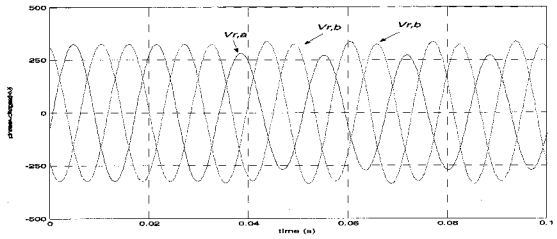

Fig. 7. Faulted phase voltages at the receiving end

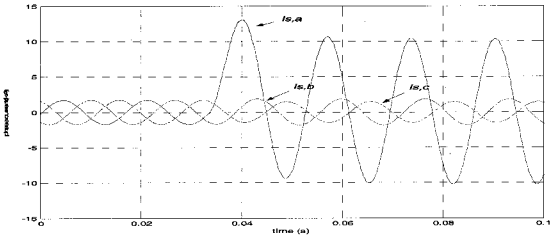

Fig. 8. Faulted phase currents at the sending end

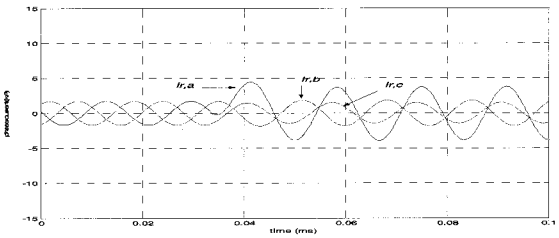

Fig. 9. Faulted phase currents at the receiving end

The arc voltage waveform and amplitude are assumed to be of square wave shape with amplitude of V_a =4.5 [kV] as shown in Fig. 10. The fault inception is 33 [ms] and fault resistance is R_F = 8 [Ω].

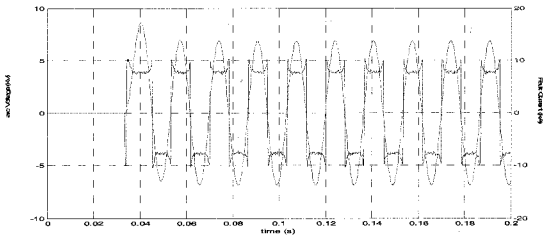

Fig. 10. Arc voltage and fault current

To investigate the impact of different synchronization errors on the estimation of the fault distance and arc voltage amplitude, six synchronization errors are tested. A

synchronization error of 0, 0.125, 0.25, 0.5, 0.75, and 1 *ms* is added to the test input data. Fig. 11 shows the fault location and the arc voltage amplitude calculated by using the proposed algorithm.

As shown in Fig. 11, the calculated fault distance and arc voltage amplitude (ℓ =10*km* and V_a=4.5*k*V) using the synchronized phasors are obtained in 20*ms* after the fault inception. Here, the relative errors for fault distance and arc voltage amplitude are less than 0.001 and 0.01%, respectively. From the calculated arc voltage amplitude, the decision as to which type of fault (transient-with arc, or permanent-without arc) occurred is obtainable before the line is tripped. Also, the results of the proposed algorithm obtained by using phasors with synchronization error are given in Fig. 11. In spite of the synchronization error, the arc voltage amplitude is calculated almost correctly.

From the algorithm speed and accuracy point of view, the results obtained confirm that the algorithm is useful for the application to actual overhead line protection.

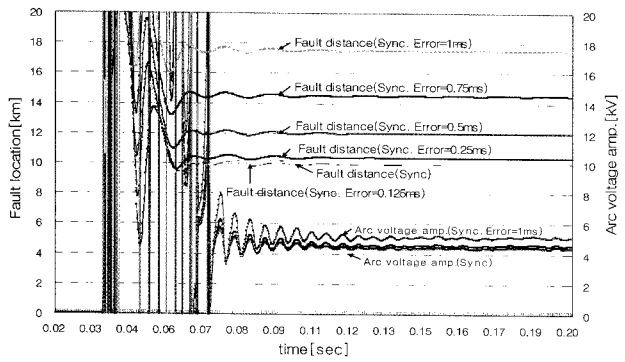

Fig. 11. Estimated fault location (exact value used by EMTP was 10 km) and arc voltage amplitude (exact value used by EMTP was 4.5 kV)

3.2 Long line application (with shunt capacitance)

In Fig. 12 the line parameters for this case are: r = 0.1 [Ω/km], x = 0.36 [Ω/km], r_0 = 0.25 [Ω/km], x_0 = 0.6 [Ω/km], c = 3.0 [μF], and c_0 = 2.0 [μF]. Sequence impedance of network A are: Z_{Ap} = 5+j13 [Ω], Z_{An} = 4+j10 [Ω], and Z_{A0} = 3+j6 [Ω]. Sequence impedance of network B are: Z_{Bp} = 5+j18 [Ω], Z_{Bn} = 4+ j14 [Ω], and Z_{B0} = 3+ j19 [Ω]. The equivalent electromotive forces of networks A and B are E_A = 133 [kV] and E_B = 100 [kV], respectively. Here, network A and B are equivalent power systems connected to the sending- and receiving ends of the transmission line.

The arc voltage used by EMTP is assumed to be of square wave shape with amplitude of V_a = 1000 [kV], corrupted by the random noise. For the medium line (200 km) and long line (300 km), results with the proposed algorithm for different fault points are shown in Tables 1 and 2. Here, the first column of the table specifies the fault location in percent from bus S. The second column is the proposed algorithm estimate using a simple lumped impedance model (without shunt) and the last column is the two-terminal estimate using a $\prod$ line model (with shunt).

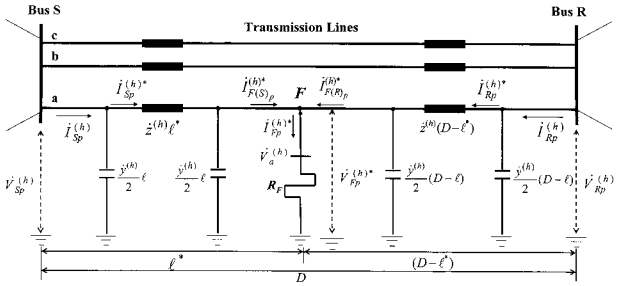

Fig. 12. Schematic of the test power system with shunt capacitance

Table 1. Two-Terminal fault location estimates for the different fault points on the line (D=200km)

Fault Point[%]	Without Shunt		With Shunt	
	Estimated[km]	Error[%]	Estimated[km]	Error[%]
20	18.4806	0.7597	20.085	0.0425
50	48.5588	0.7206	50.064	0.0320
100	100.168	0.0840	99.9191	0.0404
150	152.179	1.0895	149.713	0.1435
180	182.740	1.3700	179.613	0.1935

Table 2. Two-Terminal fault location estimates for the different fault points on the line (D=300km)

Fault Point[%]	Without Shunt		With Shunt	
	Estimated[km]	Error[%]	Estimated[km]	Error[%]
10	6.75676	1.0811	10.1896	0.0632
50	45.1420	1.6193	50.1411	0.0470
100	96.6154	1.1282	100.011	0.0037
150	150.588	0.1960	149.730	0.0900
200	205.118	1.7060	199.325	0.2250
280	287.574	2.5247	278.886	0.3713

For the medium line (200 km) and long line (300 km), Tables 3 and 4 present the results obtained by using the proposed algorithm for arc voltage amplitude at different fault points on the line. Here, the exact value of the arc voltage amplitude used by EMTP is V_a = 1000 [kV].

Table 3. Comparison of the calculated arc voltage amplitude (D=200km)

Fault Point[%]	Without Shunt	With Shunt
	Calculated Arc Vol. Amp.[kV]	Calculated Arc Vol. Amp.[kV]
20	960.420	1001.37
50	981.009	998.661
100	1017.10	997.568
150	1052.49	1003.32
180	1072.42	1009.78

Table 4. Comparison of the calculated arc voltage amplitude (D=300km)

Fault Point[%]	Without Shunt	With Shunt
	Calculated Arc Vol.Amp.[kV]	Calculated Arc Vol.Amp.[kV]
10	895.580	1006.58
50	932.487	1001.56
100	985.778	1000.48
150	1040.74	1006.58
200	1095.23	1020.43
280	1178.18	1060.23

Since the shunt capacitances (in $\prod$ model of the line) parallel to the fault resistance affect the accuracy of the fault location estimation and arc voltage amplitude calculation, accurate compensation for long lines should be considered to develop the fault algorithm. From the test results, the proposed algorithm for the fault location estimation and fault discrimination can be applied to the long line model. Through the analysis for the various case studies, when considering the shunt capacitance in a long line model, errors of unknown parameter estimation are reduced.

4. Conclusion

In this paper a new numerical algorithm for fault distance and arcing fault recognition, based on the two terminal data and derived in spectral domain, has been developed. The proposed algorithms have been derived for the case of the most frequent single-phase line to ground fault. The electric arc has been modeled with its voltage wave shape defined numerically on the basis of a number of arc voltage records.

The developed two terminal algorithms use the synchronized phasor information measured from the assumed PMUs installed at two terminals of the transmission lines. The proposed algorithm is based on the spectral analysis of the input phase voltages and line current signals measured by numerical relay. Only fundamental and third harmonic phasors calculated by Discrete Fourier Technique are needed for algorithm development. The proposed algorithm is robust and fast. Also, in spite of the synchronization error, the arc voltage amplitude was calculated correctly. From the algorithm speed and accuracy point of view, the results obtained confirm that the algorithm is useful for the application to real transmission line protection. In the case of long line model, the shunt capacitance in order to obtain the more accurate result is considered in this algorithm. Also, synchronized phasors are used to compensate for phase delay or different sampling rates of the different recording devices. The proposed algorithm for the long line model is relatively simple and easy to be implemented in the on-line application

Acknowledgements

This work was supported by the Konkuk University in 2008

References

[1] T. Takagi, et al., "Development of a new fault locator using the one-terminal voltage and current data," *IEEE Trans. on PAS*, vol. PAS-101, No. 8, pp. 2892-2898, August 1982.

[2] L. Eriksson, M. Saha, and G.D. Rockfeller, "An accurate fault locator with compensation for apparent reactance in the fault resistance resulting from remote-end in feed," *IEEE Trans. on PAS*, Vol. PAS-104, No. 2, pp. 424-436, Feb. 1985.

[3] M. Sant and Y. Paithankar, "One line digital fault locater for overhead transmission line," *IEE Proceedings*, Vol. 126, No. 11, pp. 1181-1185, Nov. 1979.

[4] Y.-H. Lin, C.-W. Liu, and C.-S. Chen, "A new PMU-based fault detection/location technique for transmission line with consideration of arcing fault discrimination-Part 1: theory and algorithm," *IEEE Trans. on Power Del.*, vol. 19, No. 4, pp. 1587-1593, Oct. 2004.

[5] Y.-H. Lin, C.-W. Liu, and C.-S. Chen, "A new PMU-based fault detection/location technique for transmission line with consideration of arcing fault discrimination-Part 2: performance evaluation," *IEEE Trans. on Power Del.*, Vol. 19, No. 4, pp. 1594-1601, Oct. 2004.

[6] J. G. McNeff, "The global positioning system," *Microwave theory and Techniques, IEEE Transaction on*. vol. 50, No. 3, pp. 645-652, March 2002.

[7] Z. Radojević, V. Terzija, M. Đurić, "Numerical Algorithm for Overhead Lines Arcing Faults Detection and Distance and Directional Protection," *IEEE Transactions on Power Delivery*, Vol. 15, No. 1, January 2000, pp. 31-37.

[8] M.Djurić, V.Terzija, "A new approach to the arcing faults detection for autoreclosure in transmission systems," *IEEE Trans. on Power Delivery*, Vol. 10, No. 4, Oct. 1995, pp. 1793-1798.

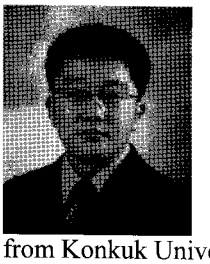

Hyun-Houng Kim
He received his B.E. degree from Jeonju University, South Korea, in 2004, and his M.S. degree from Konkuk University, South Korea, in 2006. He is currently working toward his Ph.D. in Electrical Engineering from Konkuk University.

Chan-Joo Lee
He received his B.E. degree from Anyang University, South Korea, in 2000, and his M.S. and Ph.D. degrees from Konkuk University, South Korea, in 2002 and 2006, respectively. Since 2006 he has worked as a Market Analyst in the power trading team at K-Power, Korea. His research interests are economic studies and power system planning.

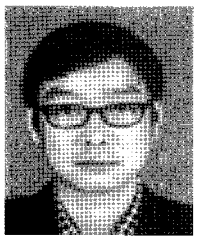

Jong-Bae Park
He received his B.E., M.S. and Ph.D. degrees in Electrical Engineering from Seoul National University, South Korea, in 1987, 1989, and 1998, respectively. From 1989-1988, he worked as a Researcher at the Korea Electric Power Corporation (KEPCO), and since 2001 he has been an Assistant Professor at Konkuk University, Korea. His research interests are power system planning and economic studies.

Joong-Rin Shin
He received his B.E., M.S., and Ph.D. degrees in Electrical Engineering from Seoul National University, South Korea, in 1977, 1984, and 1989, respectively. Since 1990, he has been with the Department of Electrical Engineering, Konkuk University in Seoul, Korea, where he is currently a Professor. His major research fields are power system analysis, power system planning, and reliability evaluation.

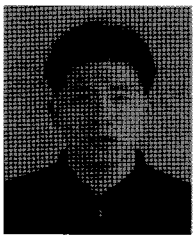

Sang-Yun Jeong
He received his B.E. and M.S. in Electrical Engineering from Konkuk University, South Korea, in 2004, 2006, respectively. He is currently working toward his Ph.D. in Electrical Engineering from Konkuk University and he is also employed at GS EPS Korea.